CHEMBIOCHEM

DOI: 10.1002/cbic.200700575

A Structural Model of the Membrane-Bound Aromatic Prenyltransferase UbiA from *E. coli*

Lars Bräuer, Wolfgang Brandt, Diana Schulze, Svetlana Zakharova, and Ludger Wessjohann*[a]

The membrane-bound enzyme 4-hydroxybenzoic acid oligoprenyltransferase (ubiA) from E. coli *is crucial for the production of ubiquinone, the essential electron carrier in prokaryotic and eukaryotic organisms. On the basis of previous modeling analyses, amino acids identified as important in two putative active sites (1 and 2) were selectively mutated. All mutants but one lost their ability to form geranylated hydroxybenzoate, irrespective of their being from active site 1 or 2. This suggests either that the two active sites are interrelated or that they are in fact only one site. With the aid of the experimental results and a new structure-based classification of prenylating enzymes, a relevant 3D model could be developed by threading. The new model explains the substrate specificities and is in complete agreement with the results of site-directed mutagenesis. The high similarity of the active fold of UbiA-transferase to that of 5-epi-aristolochene synthase (*Nicotiana tabacum*), despite a low homology, allows a hypothesis on a convergent evolution of these enzymes to be formed.*

Prenyl-converting or -transferring enzymes are responsible for the formation or modification of over 60000 naturally occurring isoprenoid-containing compounds, approximately half of which are terpenoids, while the other half are chimeric compounds of moieties from other biosynthetic origins coupled to isoprenoids (meroterpenoids). All organisms possess essential isoprenoids. The biosynthesis of this huge class of compounds is of great interest not only for biochemists and biologists, but also for medicinal and organic chemists.[1–10] Isoprenoids exhibit antimicrobial, anti-inflammatory, antiviral, and anticancer activity, with Paclitaxel (Taxol®) as one prominent example.[11–27] Chemical synthesis of terpenoids is often complicated and requires a multitude of synthetic steps.

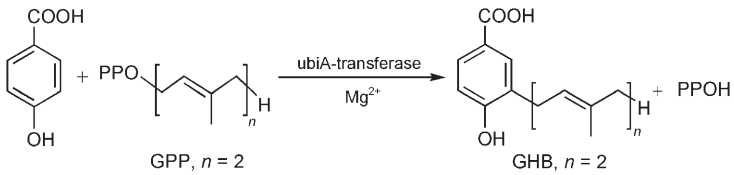

Scheme 1. Chemoenzymatic synthesis of 3-geranyl-4-hydroxybenzoate (GHB) catalyzed by UbiA-prenyltransferase ($n = 2$).

This is especially true for meroterpenoids and other chimeric compounds that demand regioselective bond formation between the isoprene moiety and the non-isoprene component. Aromatic prenyltransferases catalyze such reactions: that is, the formation of C–C bonds between an aromatic substrate and an isoprenoid diphosphate as electrophile (see, e.g., Scheme 1 for the reaction of UbiA-enzyme).[8,28]

Understanding the catalytic mechanism and modes of substrate recognition by prenyltransferases might allow new principles for chemical synthesis to be elucidated. Biosynthetic enzymes might subsequently be improved by applying structure-based rational protein design, targeted mutagenesis, or directed evolution.

Prenyl-converting enzymes are classified into terpene synthases (cyclases), prenyltransferases, isomerases, and other prenyl-converting enzymes not assigned to one of the first three groups (e.g., geranylgeranyl hydrogenase or squalene epoxidase). Prenyltransferases consist of oligoprenyl pyrophosphate synthases, protein prenyltransferases, and aromatic prenyl transferases. X-ray structures are only known for a very few prenylating enzymes. They give some insight into substrate specificity and allow the deduction of possible catalytic mechanisms. Only a single X-ray structure from the aromatic prenyltransferase class is known; however, Orf2 from *Streptomyces* sp.[29] catalyses the prenylation of a diverse set of naphthols in vitro. Its natural substrates and products are not yet known. This soluble enzyme displays a new type of antiparallel β,α-barrel fold with no structural relation to other terpene cyclases or to UbiA-transferase. In contrast to the TIM barrel, the central solvent-filled barrel of Orf2 contains binding sites for the aromatic and isoprenoid substrates. From bioinformatic analyses it is not related to most other aromatic prenyl transferases.

The membrane-bound *p*-hydroxybenzoic acid oligoprenyltransferase (UbiA) from *E. coli* consists of 290 amino acid residues encoded by the *ubiA* gene and has been known since 1972.[30] The enzyme is involved in the biosynthesis of bactoprenol and of prenylated quinones such as ubiquinone, re-

[a] *Dr. L. Bräuer, Dr. W. Brandt, D. Schulze, Dr. S. Zakharova, Prof. Dr. L. Wessjohann*
Leibniz-Institute of Plant Biochemistry
Department of Bioorganic Chemistry
Weinberg 3, 06120 Halle/Saale (Germany)
Fax: (+49) 345-5582-1309
E-mail: wessjohann@ipb-halle.de

quired for cell-wall biosynthesis and respiration, respectively. In vivo, the enzyme transfers diphosphorylated acyclic *trans*-oligoprenyl moieties (diphosphorylated terpene alcohols) to the *meta*-position of *p*-hydroxybenzoic acid (Scheme 1).[31] Despite the similar enzymatic reactions of the UbiA enzyme and the Orf2-prenyltransferase they possess different folds. Secondary structure predictions (see below) indicate an all α-helix fold for UbiA, which is membrane-bound and which could not be solubilized without irreversible destruction. As a result, no X-ray structure for UbiA or for similar (aromatic) prenyltransferases has been obtained. Similarity searches based on amino acid sequence alignments with all entries in the protein database[32] gave no relevant homologous proteins. Some years ago, we suggested a reaction mechanism and a first, tentative model of UbiA, based on the photosynthetic reaction center as template (PDB code: 1PRC, 21% amino acid sequence homology).[33] The model indicated two sequentially separated active sites, one represented by Asp71 and Asp75, and another by Asp191 and Asp195. The existence of two putative active sites was also suggested by Ashby and Edwards and by Melzer and Heide.[34,35]

Two related diphosphate-binding sites are required for isoprenoid synthases: one to activate the prenyldiphosphate, and one to fix the prolonging isopentenyl diphosphate (IPP). In theory, for (aromatic) prenyltransferases, if they are evolutionarily related, only one of these sites is required: the activating one. However, from models available at that time it remained unclear whether one site was dysfunctional, or whether both sites were still "active" sites, and whether or not they were independent of each other.

To validate the hypothesis of the existence of two sites in UbiA enzyme, site-directed mutagenesis of individual amino acid residues in the putative active sites was performed. Partial or no loss of enzyme activity on mutation of any single amino acid believed to be essential for only one of the two sites would indicate that the other site was independently active (or, in the worst case, that the mutated residues were not involved in the formation of an active site). Otherwise, an observation of complete loss of activity, irrespective of the mutation site being at active center 1 or 2 (misfolding excluded), could hint either at interdependence of the two sites or at the existence of a common site, suggesting that the preliminary model would need revision. Structural classification of a set of prenyl-converting enzymes belonging to the all α-helical protein fold family should provide insight into structural and evolutionary relationships within this group of aromatic prenyltransferases and related enzymes.

Results

Mutagenesis and enzyme activity

From the first model of the UbiA enzyme, five amino acid residues (D71, D75, R137, D191, and D195) were assumed to be crucial for catalytic activity at either of the two sites.[33] They were mutated to alanine.

By a modified method adapted from Takagi et al.,[36] the genes carrying the desired mutations were obtained by using high-fidelity DNA polymerase.[37–41] Starting from the plasmid pALMU3[35] containing the UbiA-prenyltransferase gene, the selected residues were replaced to produce the corresponding D71A, D75A, R137A, D191A, and D195A single mutants. After plasmid validation by DNA sequencing and recombinant expression of the enzymes, the catalytic activities of the mutants were compared to that of the unmodified enzyme obtained from pALMU3 expression.

All enzymes were tested for their ability to produce geranyl hydroxybenzoate (GHB) from geranyl diphosphate (GPP) in the standard assay.[31,39] Only the wild-type showed significant activity, while R137A showed strongly reduced formation of GHB, with 5% relative conversion (Figure 1).

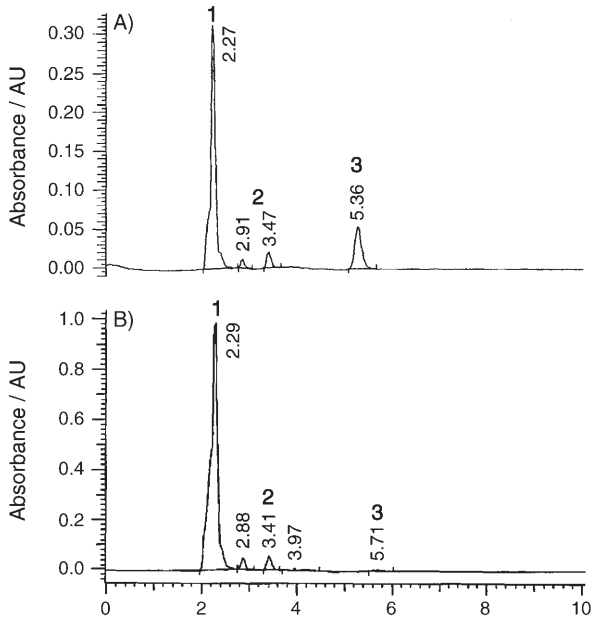

Figure 1. HPLC (254 nm) of the reaction mixture (cf. Scheme 1): 1) internal HPLC standard (*p*-hydroxybiphenyl); 2) starting material and byproducts; 3) product GHB. A) Reaction in the presence of unmodified UbiA enzyme (from pALMU3) gives GHB (3) at 5.36 min. B) R137A mutant gives reduced formation of GHB (5% rel.).

For all other mutants, no (<1%) product was observed, even on increasing the enzyme concentration. To distinguish a specific consequence of the mutation from some other effect based on misfolding, it was not possible to apply methods useful for soluble enzymes (e.g., CD spectra). However, UbiA is also able to hydrolyze GPP in the presence of $MgCl_2$ without forming GHB. This hydrolysis is not dependent on the aromatic substrate. This phosphatase activity of UbiA is overlaid by background activities of abiotic hydrolysis and of residual unspecific phosphatases, which can be present in the membrane fraction used. Fluoride unspecifically inhibits most (alkaline) phosphatases but not UbiA, unless it is used at concentrations that bind all free Mg^{2+} as fluoride. To avoid excessive MgF_2 formation, fluoride concentrations in the assay were kept below twice the $MgCl_2$ concentration. Inhibition of unspecific phos-

phatases was tested at different NaF concentrations, with a maximum of inhibitory activity found between 0.5 and 1.0 mM NaF.

Rudimentary hydrolase activity of the aromatic prenyltransferase (phosphorylase activity) with the unspecific phosphatases inhibited (Figure 2) should reflect the portion of phosphatase activity of UbiA and background hydrolysis. Abiotic background hydrolysis of GPP was determined by denaturizing the enzyme extract at 95 °C. Ideally, background hydrolysis should be equal in all samples, but different contents of proteins, salt, and buffer give variation between the different clones. In all cases, residual phosphatase activity above background levels, not due to unspecific phosphatases, was detected. Phosphatase activity stemming neither from unspecific NaF-sensitive phosphatases nor from UbiA is possible but improbable, because UbiA enzyme is known for such phosphatase activity and was highly overexpressed.

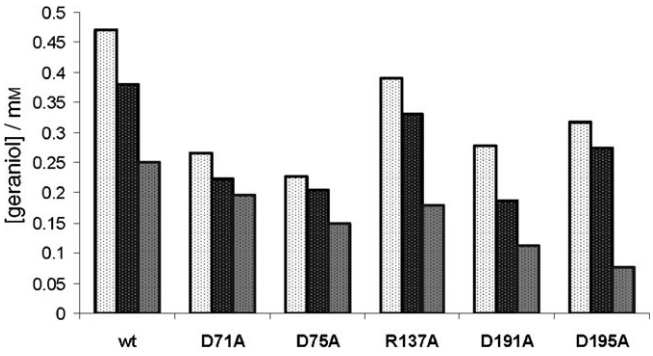

Figure 2. Degradation of geranyl diphosphate to geraniol by residual phosphatase activity of ubiA mutants and wild-type (wt at 37 °C for 2 h in the absence of 4-hydroxybenzoic acid). White columns: without phosphatase inhibitor. Dark gray columns: 1 mM concentration of NaF (phosphatase inhibitor). Light gray columns: abiotic background hydrolysis of GPP by heat-denaturized enzyme extract.

Since all aspartate mutants, irrespective of their location in putative active site 1 or 2, resulted in a complete loss of GHB formation but still showed some residual hydrolysis activity, all these residues would appear to be part of one common active site. The low activity of the R137A mutant, however, indicates that the residue is located in the vicinity of the active site, perhaps stabilizing the structure, but possibly not involved in substrate binding. The previously published active site and the UbiA protein model consequently have to be revised.

Structural classification of prenyl enzymes

On the assumption that all prenyl transfers to carbon π-systems must follow certain chemical systematics, it was hoped that there would be unrevealed evolutionary relationships between the different groups of prenylating enzymes. Some analyses of evolutionary relationships of these enzymes, such as *trans*-IPPSs and terpene cyclases, have been published.[11,40–44] For the start, all prenylating enzyme structures available from the protein database[32] were classified with the aid of the SCOP (structural classification of proteins) database.[45] The database describes structural and evolutionary relationships of proteins for which three-dimensional structures are available. The proteins are divided into domains that are subsequently classified into a hierarchy of four levels: class, fold, superfamily, and family. Each level represents a specific degree of similarity: proteins of the same superfamily often share low sequence identities, but their structural—and often also functional—characteristics suggest a probable common evolutionary origin or a convergent development from different origins. In the case of UbiA, both secondary structure and the transmembrane helix predictions suggest that it belongs to the class of all-α-helical structures. Accordingly, only this class is discussed (Figure 3).

Homology modeling of UbiA alone failed to generate a correct model because of the lack of a related X-ray structure. The structural classification of prenyl enzymes revealed similar folds, despite low sequence similarities (Figures 3 and 4). This offers the chance to model an unknown protein structure on the basis of secondary structure alignments instead of sequence alignments. This more relevant method is called threading and is available in PRIME,[46] among others.

Terpene cyclases[47] of type I are classified together with different isoprenyl pyrophosphate synthases[48] (IPPSs) such as *trans*-IPPSs and squalene synthase. Terpene cyclases of type II share a common superfamily with the β-subunit of protein prenyl transferases. Besides the structural similarity, sequences and reaction mechanisms also hint at common ancestry: both type I terpene cyclases and the IPPSs shown (not all IPPSs in general) contain aspartate-rich motifs, which overlap during structural superposition. In type I terpene cyclases and *trans*-IPPSs these motifs bind metal ions, triggering the departure of a pyrophosphate (OPP_i) leaving group,[47,48] as has been proposed for squalene synthase.[43] *trans*-IPPSs and squalene synthase each contain two aspartate-rich motifs, on helixes D and H[47] and on helixes C and H,[43] respectively, whereas type I terpene cyclases only contain the motif on helix D. A conserved sequence on helix H of type I terpene cyclases is poor in aspartate.[47]

Despite high structural similarity of type I terpene cyclases and *trans*-IPPSs the sequence identity (Figure 4) within these groups is not significantly higher than between the groups; farnesyl diphosphate synthase (FPPS) of *Staphylococcus aureus* (1RTR, group **a**), for example, is more similar to (+)-bornyl diphosphate synthase of the plant *Salvia officinalis* (1N1B, group **b**, 32.4%, 15.9%) than to FPPS of the eukaryote *Gallus gallus* (1FPS, group **a**, 29%, 23.2%). This emphasizes the independent evolution of FPPSs in prokaryotes and eukaryotes, as proposed by Bohlmann, by Meyer-Gauen and Croteau,[11] and by Tachibana et al.[41] Despite their being structurally related, the sequence identity of UbiA within the groups **a** and **b** is very low, as are the identities within this group (Figure 4). This finding, however, offers a completely new view, and an opportunity for the remodeling of UbiA through the formation of a similar fold following a classification by SCOP (Figure 3). In combination with the experimental results on substrate specif-

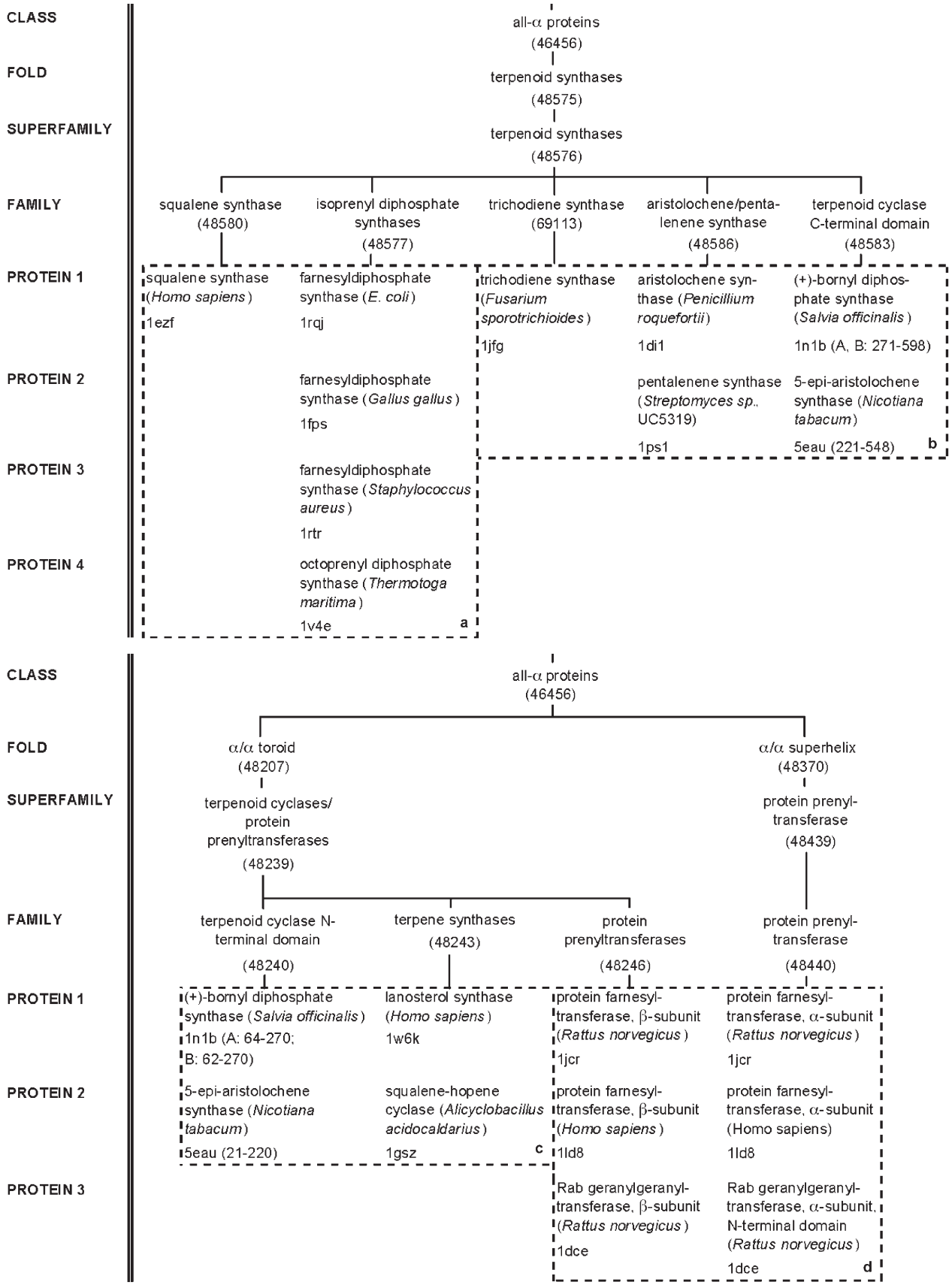

Figure 3. Classification of all-α prenyl-converting enzymes determined with the aid of the SCOP database. The numbers below each node of the trees represent the SCOP codes of a specific entry. For each enzyme a representative PDB entry is shown (e.g., 1ezf for squalene synthase from *Homo sapiens*). PDB entries can occur several times if their domains appear in different families. Boxes: **a** = IPPSs, **b** = type I terpene cyclases, **c** = type II terpene cyclases, **d** = protein prenyltransferases.

	1DI1	1JFG	1N1B	1PS1	5EAU	1FPS	1RQJ	1RTR	1V4E	1EZF	UBIA
1DI1	100.0	17.3	**29.5**	17.0	**26.0**	19.0	15.5	14.3	17.3	16.1	17.3
1JFG	15.8	100.0	**29.9**	14.7	24.3	14.2	17.9	19.5	18.7	18.4	18.7
1N1B	16.9	18.7	100.0	15.7	**31.8**	14.7	14.9	15.9	11.9	16.4	12.2
1PS1	17.2	16.3	**27.9**	100.0	**28.5**	18.7	16.0	14.5	14.2	24.3	14.8
5EAU	16.2	16.6	**34.7**	17.5	100.0	16.6	12.6	14.8	13.7	18.1	12.0
1FPS	17.7	14.4	24.0	17.2	24.8	100.0	22.3	23.2	21.8	16.6	19.1
1RQJ	17.7	22.4	**29.8**	18.1	23.1	**27.4**	100.0	**40.5**	**27.8**	21.7	15.1
1RTR	16.7	24.9	**32.4**	16.7	**27.6**	**29.0**	**41.3**	100.0	**27.6**	21.2	17.1
1V4E	19.7	23.4	23.7	16.1	**25.1**	**26.8**	**27.8**	**27.1**	100.0	24.1	17.4
1EZF	13.2	16.5	23.5	19.7	23.7	14.6	15.6	14.9	17.3	100.0	13.9
UBIA	20.3	24.1	**25.2**	17.2	22.8	24.1	15.5	17.2	17.9	20.0	100.0

Figure 4. Residue identities of pairwise alignments of prenyltransferases from Figure 3 **a**, **b** and UbiA with use of BLOSUM30 as substitution matrix (gap costs: start = 7, gap extent = 1). The alignment of two sequences produces two scores: values above the diagonal of the matrix give results of the substitution matrix divided by the length of the chain in the rows, values below the diagonal are formed by dividing by the length of the chain in the column. 1DI1: aristolochene synthase (*Penicillium roqueforti*), 1JFG: trichodiene synthase (*Fusarium sporotrichioides*), 1N1B: (+)-bornyl diphosphate synthase, chloroplast enzyme (*Salvia officinalis*), 1PS1: pentalenene synthase (*Streptomyces* sp., strain UC5319, 5EAU: 5-epi-aristolochene synthase (*Nicotiana tabacum*), 1FPS: farnesyl pyrophosphate synthetase (*Gallus gallus*), 1RQJ: farnesyl pyrophosphate synthetase (*Escherichia coli*), 1RTR: farnesyl pyrophosphate synthetase (*Staphylococcus aureus*, strain MW2), 1V4E: putative octoprenyl-diphosphate synthase (*Thermotoga maritima*), 1EZF: squalene synthetase (*Homo sapiens*), UBIA: 4-hydroxybenzoate oligoprenyltransferase (*Escherichia coli*); gray highlighted background: upper left area = type I terpene cyclases, lower right area = IPPSs; bold values mark sequence identities above 25%.

icity and on amino acid mutagenesis this gives a starting point to generate a reasonable structural model of UbiA.

Modeling of UbiA enzyme

Threading started with prediction of the secondary structure of the protein to be modeled by the standard secondary structure prediction method implemented in PRIME (SSpro).[49] From the predicted similar structures, the prenylating enzyme 5-epi-aristolochene synthase from *Nicotiana tabacum* (PDB code: 5EAU) proved to be the most promising template for modeling of UbiA (see the Experimental Section).[50] The secondary structure prediction and the predicted transmembrane helices (Ps*i*Pred server[51,52] and MEMSAT3[53–55]) for UbiA aligned with the actual secondary structure of 5-epi-aristolochene synthase are shown in Figure 5. In contrast to UbiA, 5-epi-aristolochene synthase is not a membrane-bound enzyme, and according to the SCOP classification it consists of two domains: an N-terminal domain (Figure 2, family 48240), and a C-terminal domain (family 48583) starting at amino acid residue K221 and including the catalytically active site. The secondary structure alignment starts with E243 and ends at N523 of the template (cf. Figure 5, corresponding to UbiA residues number 4 to 271, respectively). In the X-ray structure, this sequence is followed by an unresolved gap of five amino acids. Except for a small helix at position 149–156 (numbering for UbiA is used), all predicted helices for UbiA agree with those of the X-ray structure of 5-epi-aristolochene synthase. The catalytically active site for the recognition of the pyrophosphate of the substrate of 5-epi-aristolochene synthase is formed by the amino acid residues D301 and D305, both

```
          1                                                  49
5EAU: ~~~ELAQVSRWWKDLDFVTTLPYARDRVVECYFWALGVYFEPQYSQ~~~~
UBIA: MEWSLTQNKLLAFHRLMRT~DKPIGALLLLWPTLWALWVATPGVPQLWIL
SS-5: ~~~~-HHHHHHHHH-------------HHHHHHHHHHH------HH~~~~
SS-U: ~~~~~-HHHHHHHH-----------------HHHHHHHHH-----------

         50                  71                          87
5EAU: ~~~~~~ARVMLVKTISMISIVDDTFDAYGTVKELEAYTDAIQRWDINEID
UBIA: AVFVAGVWLMRAAGCVVNDYADRKFD~~~~~~~~~~GHVKRTANR~~PLP
SS-5: ~~~~~~HHHHHHHHHHHHHHHHHHHH----HHHHHHHHHHHHH-------
SS-U: -----HHHHHHHHHHHHHHHHHHHH-~~~~~~~~~~~-HHHHHH-------

       88                                                137
5EAU: RLPDYMKISYKAILDLYKDYEKELSSAGRSHIVCHAIERMKEVVRNYNVE
UBIA: SGAVTEKEARALFVVLVLISFLLVLTLNTMTILLSIAALALAWVYPFMKR
SS-5: ----HHHHHHHHHHHHHHHHHH---------HHHHHHHHHHHHHHHHHH
SS-U: ---HHHHHHHHHHHHHHHHHH---------HHHHHHHHHHHHHHHHHH

      138                                               171
5EAU: STWFIEGYTPPVSEYLSNALATTTYYYLATTSYLGMKSATEQDFEWLSKN
UBIA: YTH~~~~~~LPQVVLG~~AAFGWSIPMAFAAV~SESVP~~~~~~~~LSCW
SS-5: HHHHHH------HHHHHHH-----HHHHHHHHHH------HHHHHHHH--
SS-U: HH-~~~~~~~~~~~~~~~~~~~~HHHHHHH-~~~~~~~~~~~~~~~~~~

      172                 191                           228
5EAU: PKILEASVIICRVIDDTATYEVEKS~RGQIATGIECCMRDYGISTKEAMA
UBIA: LMFLANILWAVAYDTQYAMVDRDDDVKIGIKS~~~TAILFGQYDKLIIGI
SS-5: --HHHHHHHHHHHHHHHH-HHHHH-~~~~~~~HHHHHHHHH---HHHHHH
SS-U: -HHHHHHHHHHHHHHHHH-HHHHHH-----------~~~~-HHHHH---HHHHHH

      229                                               270
5EAU: KFQNMAETAWKDINEGLLRPTPVSTEFL~~~~~~~TPILNLARIVEVTYI
UBIA: LQIGVLALMAIIGELN~~~~~~~~GLGWGYYWSILVAGALFVYQQKLIAN
SS-5: HHHHHHHHHHHHHHHH----------~~~~~~~HHHHHHHHHHHHH--
SS-U: HHHHHHHHHHHHHHHH-~~~~~~~~~~~~~~~~~~~HHHHHHHHHHH--

      271                          300
5EAU: HN
UBIA: REREACFKAFMNNNYVGLVLFLGLAMSYWHF
```

Figure 5. Alignment of the amino acid sequence of 5-epi-aristolochene synthase (5EAU) for the domain 243–523 with that of UbiA based on secondary structure alignment (H = helix, in rows SS-5 the actual secondary structure of 5EAU, and in rows SS-U the helical structure of ubiA predicted by PRIME and SSpro). The residues of the proposed active site are highlighted in bold, while the residues subjected to site-directed mutagenesis are underlined.

complexing one magnesium cation, D444 and E452 binding a second magnesium cation, and R264 (highlighted in Figure 5). There is another glutamate (E379) in close proximity to the pyrophosphate binding site that shows no direct interaction with the diphosphate moiety.

All the aspartate residues mutated in UbiA appear relevant for substrate or Mg^{2+} binding on consideration of the new template. From this alignment, a revised model of UbiA was developed with PRIME. A PROCHECK[56] analysis of the resulting structure, after energy and loop refinement with the OPLS force field of PRIME,[57] gave a Ramachandran plot with only 74% of the residues in most favored areas and six in disallowed regions. The model was therefore refined again with CHARM M22[58] with the Born solvation model[59] implemented in MOE.[60] Three remaining outliers in disallowed regions of amino acid residues in the Ramachandran plot occurring in loop regions outside the active site were corrected manually. Finally, PROCHECK analysis showed 87.6% backbone dihedral angles in most favored regions, 11.2% in additionally allowed, and 1.2% in generously allowed regions, planarity of the peptide bonds, realistic hydrogen bond energies, and side chain dihedral angle distributions. PROSA analysis[61] is based on statistical analyses of several distances (e.g., C_β–C_β distances) of X-ray structures of proteins. A potential of mean force was derived and used to evaluate the suggested folding of the UbiA model (Figure 6). Except for the N- and C-terminal parts, the energy profiles of the two proteins are similar. While the N terminus of the model of UbiA shows a more negative energy, the opposite can be seen at the C terminus of the template. The overall negative and similar energy profile for the two potentials indicates that the model of UbiA represents a reasonable native-like fold, especially in the central region, where the active site is located.

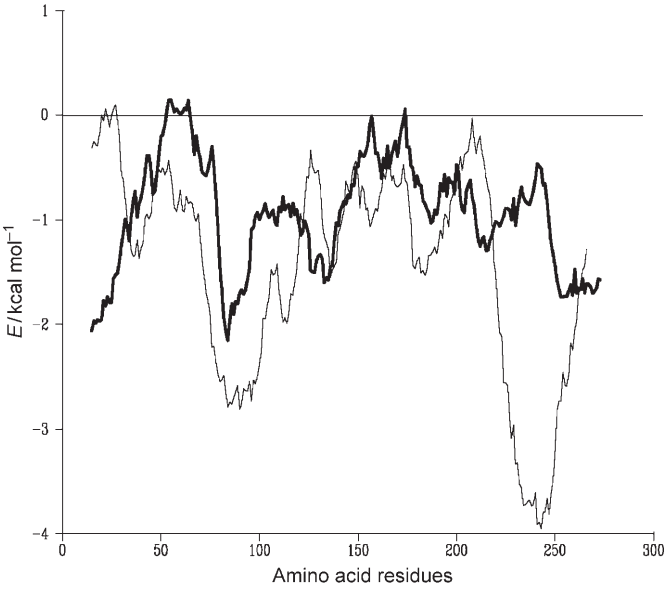

Figure 6. PROSA plot of the template 5-epi-aristolochene synthase fragment 243–523 (thin line) in comparison with the model of ubiA (bold line).

The secondary structure of the model of UbiA (Figure 7, inside top view), includes the ligand in the active site. The putative location in the membrane is displayed in Figure 8.

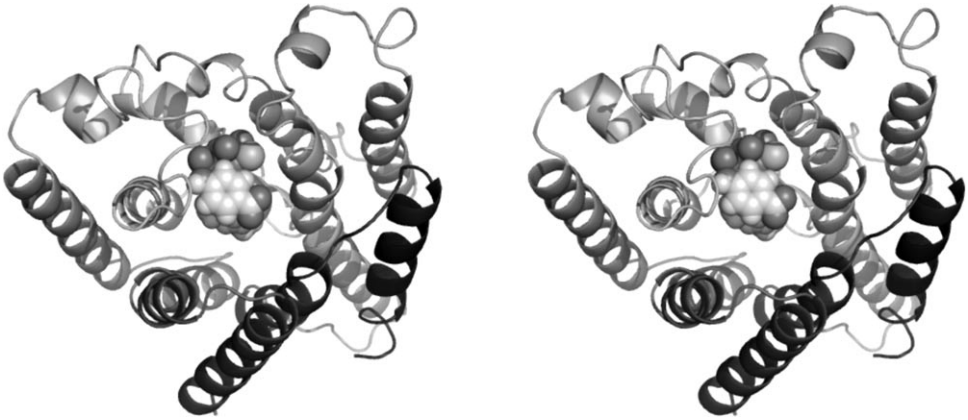

Figure 7. Stereorepresentation of the secondary structure, giving an inside top view of UbiA-prenyltransferase with the docked substrates 4-hydroxybenzoate (PHB) and geranyl pyrophosphate (hidden under PHB; only the phosphates can partially be seen) The activated electrophilic prenyl residue appears ideally shielded from water hydrolysis by PHB.

The lipophilic potential at the Connolly surface (Figure 9) shows a deep lipophilic binding pocket for the prenyl chain but also a predominantly lipophilic potential at the outer surface of the protein, in order to locate it within the membrane. The active site of UbiA was compared to the template 5-epi-aristolochene synthase with both substrates included (Figure 10). Geranyl pyrophosphate is bound to UbiA in a similar way as the non-native substrate trifluorofarnesyl diphosphate in 5-epi-aristolochene synthase. The pyrophosphate group is complexed through a magnesium cation, which itself is bound by the two aspartates 71 and 75. Whereas the P_α-phosphate group of the template forms a salt bridge with Arg264 (right side), Arg137 in UbiA replaces the second magnesium dication of the template protein and recognizes the P_α-phosphate group through hydrogen/ion pair bonding. Salt bridges with Asp191 and Asp195 fix the conformation of Arg137 itself. Only these slight differences between the active sites of the two proteins cause Arg72 to be able to bind the carboxylic acid group of the second substrate, *p*-hydroxybenzoate, which does not need to be accommodated in the template. Unlike in the template, Asp191 is available for a new function. It supports binding and activation of the second substrate through H-bonding to the phenolic hydroxy group.

The geranyl moiety is located in a hydrophobic pocket and mainly recognized by the electron-rich Trp152, which is ideally

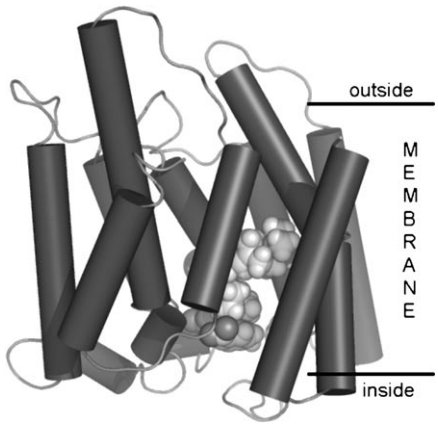

Figure 8. UbiA secondary and tertiary structure side view with putative location of the membrane. Substrates 4-hydroxybenzoate (PHB) and geranyl pyrophosphate are located in the centre of the membrane bundle.

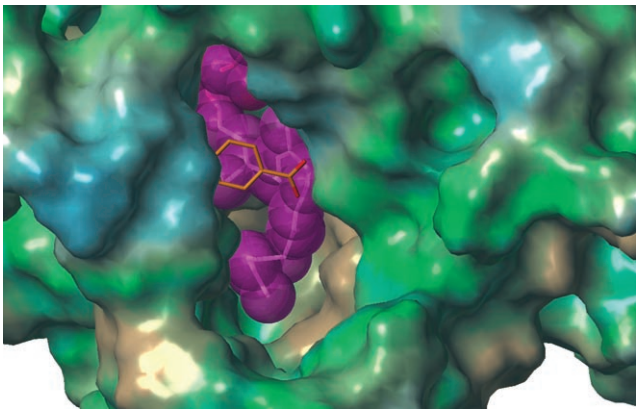

Figure 9. All-*trans*-geranylgeranyl pyrophosphate in the proposed active site of UbiA with lipophilic potential at the Connolly surface. The brown areas deep in the binding pocket show the stabilizing hydrophobic interactions between the prenyl ligand and the enzyme, also leaving space for longer prenyl chains. The aromatic substrate clearly shields the activated prenyl cation from water attack.

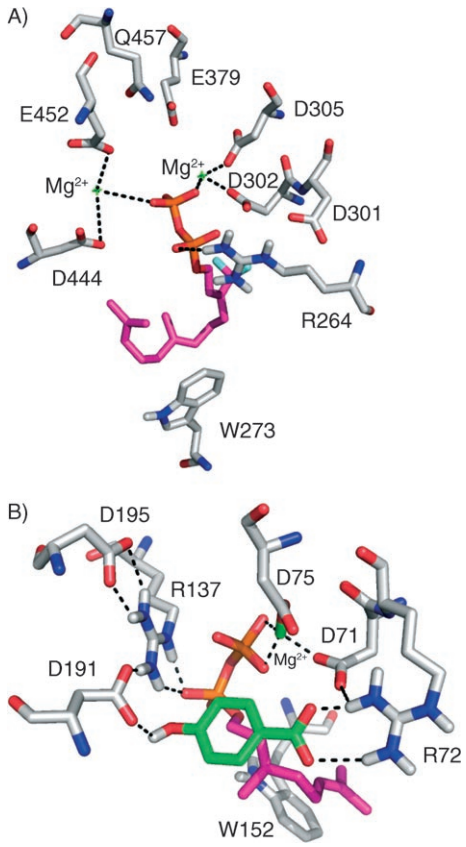

Figure 10. A) Active site of the template X-ray structure of 5-epi-aristolochene synthase (atom-typed) with the artificial ligand trifluorofarnesyl diphosphate (magenta). B) Active site of the UbiA model (atom-typed) with *p*-hydroxybenzoate (green) and geranyl pyrophosphate (magenta). For clarity, all hydrogen atoms not essential for substrate recognition are omitted.

positioned to stabilize an intermediate allylic cation formed after diphosphate abstraction (in a similar way as in the template protein; cf. Figure 10 A and B),. Additionally, the first isoprene moiety of geranyl pyrophosphate stabilizes the binding and orientation of the *p*-hydroxybenzoate in the active site. In this position, *p*-hydroxybenzoate is ideally placed for reaction with the activated isoprenyl residue. The prenyl C_α atom bound to the pyrophosphate is in close proximity to the *meta*-position of *p*-hydroxybenzoate perpendicular to the aromatic ring system; that is, it has an ideal overlap with the π-orbitals. Proton transfer from the hydroxy group of *p*-hydroxybenzoate to Asp191 would enhance the negative partial charge at the *meta*-position and initiate the catalytic reaction.[33] Subsequent or concerted cleavage of the pyrophosphate from the isoprenyl residue would be supported by proton transfer from Arg137 to the pyrophosphate P_α. Attack of the C_α atom of the isoprene to the aromatic ring would form a σ-complex. Proton transfer from the *meta*-proton of *p*-hydroxybenzoate to the P_β-phosphate group would complete the reaction. Mechanistic details and substrate specificity of *p*-hydroxybenzoic acid derivatives have already been explained on the basis of quantum mechanical calculations.[33] The new protein model and reaction model support those calculations.

The mutational studies (cf. Figure 2) showed a detrimental effect for the mutants D71A and D75A. The model indicates that both are responsible for the fixation of the magnesium ion and with this, the recognition of the diphosphate. Mutations of Asp191, Arg137, and Asp195 to alanine also resulted in significant losses of activity, which are now equally well explained. Aspartate 191 directly binds to the *p*-hydroxybenzoate and likely activates the intermediate phenolate. The influence of Asp195 is indirect, through stabilization of the side chain of Arg137, which itself forms a salt bridge with the disphosphate and thus contributes to the recognition and correct positioning of the prenyl substrate relative to *p*-hydroxybenzoate. All results of the mutations are now consistent with the model and indicate that one unique active site is formed by two sequentially distant parts.

With longer chain length (e.g., farnesyl pyrophosphate, geranylgeranyl pyrophosphate) the reaction velocity decreased.[28,62] Longer oligoprenyl diphosphates in vitro might be less soluble or might form micelles or vesicles.[28,62–65] Octaprenyl pyrophosphate is one of the natural substrates of UbiA, involved in

ubiquinone biosynthesis,[66] and can be docked to the active site of UbiA similarly to geranylgeranyl pyrophosphate (Figure 11). In a back-folded conformation of the substrate, a multitude of hydrophobic amino acid residues of the enzyme can interact with long substrates and may cause decreased reaction velocity by slower diffusion.

Several geranyl-derived ligands have been synthesized and tested by Fulhorst et al.[62] Removal even of the distal C-7 methyl group from geranyl pyrophosphate or the reduction of the distal C-6 double bond reduced the conversion rate to about 32% of that of geranyl pyrophosphate. Doing the same at the diphosphate-proximal C2 double bond resulted in total loss of activity. The proximal isoprene group of geranyl pyrophosphate is recognized ideally by the side chain of W152. In 5-epi-aristolochene synthase, the substrate is recognized in a nearly identical manner but with a spatially differently located tryptophane. Interactions of isoprene moieties with aromatic side chains are commonly observed in X-ray structures of proteins (e.g., 1KZO, 1LTX, or 1N4P). Ab initio calculations with JAGUAR[67] and a 6-31G** basis set predicted a considerable interaction energy of 30.6 kJ mol^{-1} between an indole and a dimethylallyl unit. This indicates that aromatic rings can offer specific recognition properties for isoprenoid chains. Thus, any modification, such as removal of the C-3 methyl or C-2 double bond at the proximal isoprene unit of geranyl pyrophosphate would either reduce the affinity to the enzyme or cause a change in the electronic stabilization or the docking conformation (e.g., by reduction of the double bond), thus disturbing the ideal positioning of the activated prenyl for a reaction with *p*-hydroxybenzoate. In addition, such changes would result in significantly reduced electronic stabilization of an intermediate cationic charge. Insertion of any hydrophilic group close to the diphosphate, such as ether or ester groups in geranyl derivatives, would lead to severe or complete loss of activity because a stabilizing hydrophobic interaction and the cationic interaction with tryptophan would be prevented or strongly reduced. In concordance, the hydrophilic all-*trans*-8-(2-methylaminobenzoyloxy)-3,7-dimethyl-2,6-octadienyl diphosphate showed a conversion rate of 19% relative to geranyl pyrophosphate. In this case, the aromatic moiety can interact with Asp184 and Arg262, located deeper in the binding pocket (Figure 12). Also, more modifications are tolerated with increasing distance from the diphosphate.[62]

Discussion and Conclusions

A new protein model of the oligoprenyl *p*-hydoxybenzoate transferase (UbiA) from *E. coli* has been developed, placing the enzyme in the SCOP family 48583. The model is supported by quality analyses with theoretical methods and by site-directed mutagenesis and by its classification of prenyl-converting enzymes based on 3D structural alignments (SCOP), and it explains the most important aspects of substrate specificity. The proposed structure represents the first 3D structure of a membrane-bound aromatic prenyltransferase. The earlier suggestion of the existence of two independent catalytic active sites must be discarded. The very low sequence homology of UbiA with other isoprenoid-converting enzymes, but also the (contradicting) existence of two typical active site elements common to such enzymes—here combined to one site only—suggest a convergent evolution. This may have started from an early ancestor isoprenoid prolongation enzyme with the typical two substrate sites, with subsequent evolution into a "one-substrate" enzyme as in terpene cyclases, which possess similar "united" active sites. Eventually, further modifications would have allowed access and conversion of a nonisoprenoid second substrate.

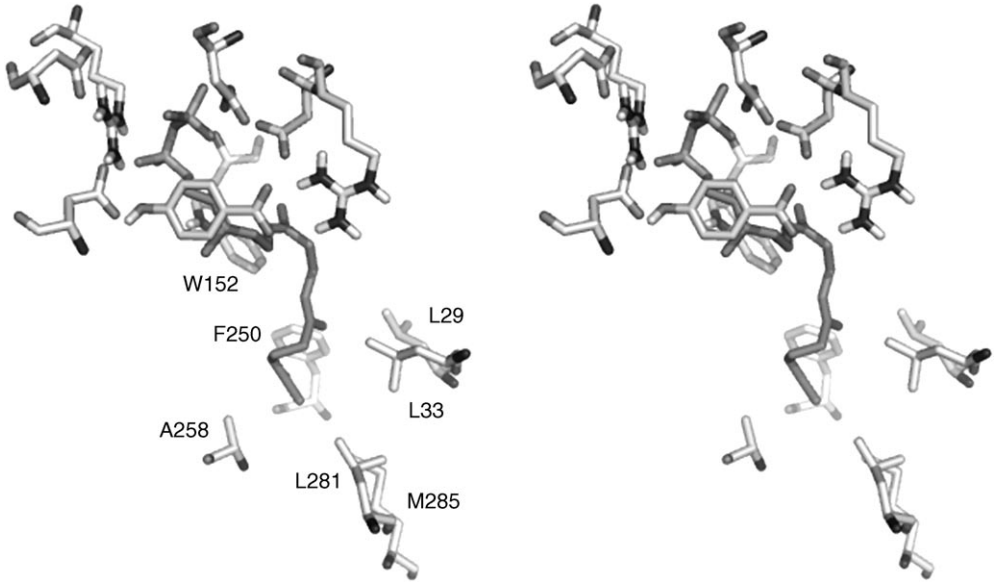

Figure 11. Stereoview of all-*trans*-geranylgeranyl pyrophosphate docked to the active site of UbiA. The hydrophobic tail of the prenyl substrate is bound by several hydrophobic amino acid residues.

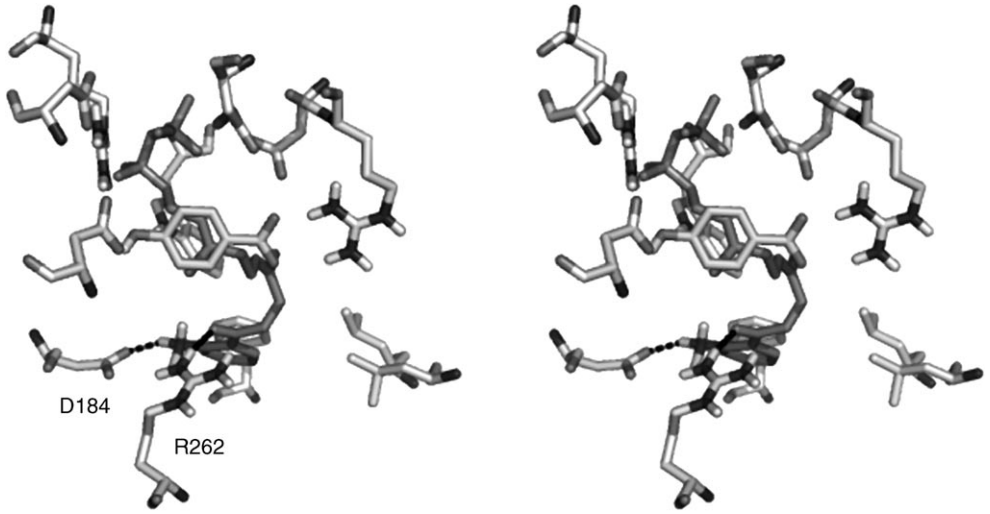

Figure 12. Stereoview of the docking arrangement of all-*trans*-8-(2-methylamino-benzoyloxy)-3,7-dimethylocta-2,6-dienyl diphosphate, showing the interactions with Asp184 and Arg262.

Experimental Section

Chromatography: HPLC (Lichrosphere 100, 5 μm RP 18) was performed on a Merck D-7000 instrument with integrated photo diode array detector. Samples were chromatographed with methanol/water mixtures 80:20 containing formic acid (0.2%), flow rate: 1 mL min^{-1}. GC-MS spectra were performed on a MD800 GC 8000 (Fisons Instruments, column DB-5MS: J&W 20 m × 0.25 mm, 0.25 μm film thickness). The probes were measured at 70 eV EI, source temperature 200 °C, injection temperature 250 °C, interface temperature 300 °C, carrier gas He, flow rate (0.8 mL min^{-1}), splitless injection. Temperature program: start at 40 °C, hold for 5 min, raise to 180 °C at 10 °C min^{-1}, raise to 290 °C at 50 °C min^{-1}, hold at 290 °C for 3 min.

A) Prenyltransferase assay (standard, GHB formation): For the activity assays, unlabeled GPP was produced in two steps from geraniol.[68] Diethyl ether was freshly distilled from sodium/benzophenone. Other solvents and chemicals obtained from commercial sources were used without purification. The 1 mM assay contained in a final volume (100 μL, 10 μL) of a 10 mM *p*-hydroxybenzoic acid solution; (10 μL DMSO; 10 μL 10 mM $MgCl_2$; 10 μL 10 mM) geranyl diphosphate, and 50 μL enzyme preparation in 50 mM Tris/HCl buffer (pH 7.8 in 10 mM 1,4-dithioerythrol) filled to 100 μL total assay volume with 50 mM Tris/HCl of pH 7.8 (i.e., 10 μL). After incubation for 2 h (37 °C, shaking), the reaction was stopped by addition of aqueous formic acid (2%, 20 μL). Products were extracted with ethyl acetate (0.5 mL), which was removed in vacuo, and the remainder was dissolved in methanol (100 μL), containing *p*-hydroxybiphenyl (25 μM) as an internal HPLC standard. The samples were analyzed for the formation of GHB by HPLC.

B) Prenyltransferase assay (geraniol formation, phosphatase inhibition): The enzyme preparation contained a suspension of membrane-bound protein in tris-HCl buffer (pH 7.8, in 10 mM DTT). NaF solution (10 mM, 10 μL, 100 nmol, in 50 mM Tris-HCl buffer, pH 7.80), $MgCl_2$ solution (10 mM, 10 μL, 100 nmol, in 50 mM Tris-HCl buffer, pH 7.80), the enzyme preparation (50 μL), Tris-HCl buffer (50 mM, pH 7.80, 10 μL), and DMSO (10 μL) were placed in a 1.5 mL Eppendorf tube. Finally, a GPP solution (10 mM, 10 μL, 100 nmol, in 50 mM Tris-HCl buffer, pH 7.80) was added. The resulting mixture (final volume of 100 μL) was incubated at 37 °C. After 2 h, the aqueous layer was extracted with ethyl acetate (500 μL). After rapid centrifugation at 4000 rpm, the organic layer was partially (450 μL) transferred to a 1 mL vial and concentrated to dryness under reduced pressure. The evaporation residue was dissolved in methanol (100 μL), containing limonene as an internal standard, and analyzed by GC-MS. The formed geraniol was quantified with the aid of a geraniol calibration curve.

Mutagenesis and protein expression: All site-directed mutagenesis experiments used PCR with AccuPrime Pfx Supermix (Invitrogen).[36,38,69] For the production of the single mutants, the procedure was performed with use of the pALMU3-vector as template.[35,70] For replication and expression of the genes, the mutated constructs were cloned by transforming them into competent *E. coli* DH10B cells (Invitrogen), as an intermediate step. All mutated constructs were validated and approved by sequencing (MWG Biotech AG, Ebersberg, Germany). The transformed cells were grown at 37 °C in LB medium (500 mL) supplemented with ampicillin (50 μg mL^{-1}). When the OD_{600} of the medium was between 0.9 and 1.5, the gene expression was stopped without further induction. The cells were harvested by centrifugation at 5000 rpm for 10 min. The bacterial pellet was resuspended in Tris/HCl buffer (50 mM, pH 7.8 in 10 mM 1,4-DTT, pH 7.8) and lysed by treatment in a French press. All washing and lysis steps were carried out at 4 °C. The membrane fraction containing the UbiA-enzyme was concentrated by ultracentrifugation at 40000 rpm and resuspended in Tris/HCl (50 mM, 10 mM DTT buffer, pH 7.8).

Molecular modeling and bioinformatics: All relevant protein structures from the protein database[32] were classified with SCOP[45] (structural classification of proteins; release 1.71). Homology modeling was performed with the aid of threading and SSpro available in PRIME of Schrödinger's modeling software tools.[46,49] From this secondary structure prediction, proteins with experimental structures showing the greatest similarity were selected. Two of the predicted structures appeared to belong to the group of prenyl enzymes of the all-α-domain class assigned by the SCOP analysis.

These are a pentalenene synthase from *Streptomyces* sp. UC5319 (PDB code: 1PS1)[44] and a 5-epi-aristolochene synthase from *Nicotiana tabacum* (PDB code: 5EAU).[50] For both templates, models of UbiA have been created with PRIME. However, from the alignment

of the secondary structure elements and the known active site of the pentalenene synthase it became obvious that a model based on this template cannot be of relevance for UbiA and is therefore not discussed further.

The model based on 5-epi-aristolochene synthase was refined by CHARMM22[58] with the Born solvation model[59] implemented in MOE.[60] The stereochemical quality of the model was verified with PROCHECK.[56] An analysis with PROSA II is a strong test of whether the model represents a native-like fold or not.[61] Since UbiA is a membrane-bound protein, only C_α- and C_β-potentials were used in the PROSA II analysis. The additionally available surface potentials parameterized in PROSA II are only valid for soluble proteins and are therefore irrelevant for UbiA. Geranyl pyrophosphate as the basic substrate and a magnesium cation were manually placed into the active site by reference to the corresponding arrangement of the substrate in the 5-epi-aristolochene synthase, and this was followed by 10 ps molecular dynamics simulation for relaxation and final energy minimization of the complex. During this simulation, the protein structure was completely fixed, except for those side chains pointing into the active site.

Finally 4-hydroxybenzoate was docked with GOLD (Genetic Optimized Ligand Docking, Cambridge Crystallographic Data Centre, 1998, Cambridge, UK) with standard parameter settings.[71–74] The structure can be downloaded from the internet from http://www.ipb-halle.de/tools-and-databases/protein-models/. Molecular graphics figures were created with Pymol[75] and the molecular surface potentials with MOLCAD[76] with the aid of the modeling package SYBYL.[77]

Abbreviations: PHB, 4-hydroxybenzoic acid; GPP, geranyl diphosphate; GHB, geranyl hydroxybenzoate; PCR, polymerase chain reaction; ORF, open reading frame; UbiA, 4-hydroxybenzoic acid oligoprenyltransferase encoded by the *ubiA* gene from *E. coli;* IPPS, isoprenyl pyrophosphate synthase; FPPS, farnesyl diphosphate synthase.

Acknowledgements

We thank HWP of the state of Saxony–Anhalt and the Deutsche Forschungsgemeinschaft within the framework of the priority program 1152 "evolution of metabolic diversity", grant Br1329/10-1 for financial support, Lutz Heide for the plasmid pALMU3, and Birgit Dräger, Kazufumi Yazaki, and especially Marco-Aurelio Dessoy for many valuable discussions and suggestions.

Keywords: mutagenesis · phosphatase activity · protein models · threading · transferases

[1] S. Lee, C. D. Poulter, *J. Am. Chem. Soc.* **2006**, *128*, 11545–11550.
[2] Z. Wu, J. Wouters, C. D. Poulter, *J. Am. Chem. Soc.* **2005**, *127*, 17433–17438.
[3] D. T. Fox, C. D. Poulter, *Biochemistry* **2005**, *44*, 8360–8368.
[4] L. M. Eubanks, C. D. Poulter, *Biochemistry* **2003**, *42*, 1140–1149.
[5]]W. Brandt, M. A. Dessoy, M. Fulhorst, W. Y. Gao, M. H. Zenk, L. A. Wessjohann, *ChemBioChem* **2004**, *5*, 311–323.
[6] S. B. Richard, A. M. Lillo, C. N. Tetzlaff, M. E. Bowman, J. P. Noel, D. E. Cane, *Biochemistry* **2004**, *43*, 12189–12197.
[7] S. B. Richard, J. L. Ferrer, M. E. Bowman, A. M. Lillo, C. N. Tetzlaff, D. E. Cane, J. P. Noel, *J. Biol. Chem.* **2002**, *277*, 8667–8672.
[8] C. D. Poulter, E. A. Mash, J. C. Argyle, O. J. Muscio, H. C. Rilling, *J. Am. Chem. Soc.* **1979**, *101*, 6761–6763.
[9] S. Sauret-Gueto, P. Botella-Pavia, U. Flores-Perez, J. F. Martinez-Garcia, C. San Roman, P. Leon, A. Boronat, M. Rodriguez-Concepcion, *Plant Physiol.* **2006**, *141*, 75–84.
[10] S. Takahashi, T. Koyama, *Chem. Rec.* **2006**, *6*, 194–205.
[11] J. Bohlmann, G. Meyer-Gauen, R. Croteau, *Proc. Natl. Acad. Sci. USA* **1998**, *95*, 4126–4133.
[12] S. L. Cole, R. Vassar, *Neurobiol. Dis.* **2006**, *22*, 209–222.
[13] S. J. McTaggart, *Cell. Mol. Life Sci.* **2006**, *63*, 255–267.
[14] K. M. Swanson, R. J. Hohl, *Curr. Cancer Drug Targets* **2006**, *6*, 15–37.
[15] F. Bouvier, A. Rahier, B. Camara, *Prog. Lipid Res.* **2005**, *44*, 357–429.
[16] N. Ferri, R. Paoletti, A. Corsini, *Biomarkers* **2005**, *10*, 219–237.
[17] E. Swiezewska, W. Danikiewicz, *Prog. Lipid Res.* **2005**, *44*, 235–258.
[18] R. Barkovich, J. C. Liao, *Metab. Eng.* **2001**, *3*, 27–39.
[19] P. A. Edwards, J. Ericsson, *Curr. Opin. Lipidol.* **1998**, *9*, 433–440.
[20] K. H. Altmann, J. Gertsch, *Nat. Prod. Rep.* **2007**, *24*, 327–357.
[21] D. G. I. Kingston, D. J. Newman, *Curr. Opin. Drug Discovery Dev.* **2007**, *10*, 130–144.
[22] L. Wessjohann, *Angew. Chem.* **1994**, *106*, 1011–1013; *Angew. Chem. Int. Ed. Engl.* **1994**, *33*, 959–961.
[23] J. Dubois, *Expert Opin. Ther. Pat.* **2006**, *16*, 1481–1496.
[24] D. T. Bergstralh, J. P. Y. Ting, *Cancer Treat. Rev.* **2006**, *32*, 166–179.
[25] S. H. Chen, J. Hong, *Drugs Future* **2006**, *31*, 123–150.
[26] V. Srivastava, A. S. Negi, J. K. Kumar, M. M. Gupta, S. P. S. Khanuja, *Bioorg. Med. Chem.* **2005**, *13*, 5892–5908.
[27] R. J. Hohl, *Adv. Exp. Med. Biol.* **1996**, *401*, 137–146.
[28] L. Wessjohann, B. Sontag, M. A. Dessoy in *Bioorganic Chemistry Highlights and New Aspects* (Eds.: U. Diederichsen, T. K. Lindhorst, B. Westermann, L. A. Wessjohann), Wiley-VCH, Weinheim, **1999**, pp. 79–88.
[29] T. Kuzuyama, J. P. Noel, S. B. Richard, *Nature* **2005**, *435*, 983–987.
[30] I. G. Young, F. Gibson, R. A. Leppik, J. A. Hamilton, *J. Bacteriol.* **1972**, *110*, 18–25.
[31] L. Wessjohann, B. Sontag, *Angew. Chem.* **1996**, *108*, 1821–1823; *Angew. Chem. Int. Ed. Engl.* **1996**, *35*, 1697–1699.
[32] H. M. Berman, J. Westbrook, Z. Feng, G. Gilliland, T. N. Bhat, H. Weissig, I. N. Shindyalov, P. E. Bourne, *Nucleic Acids Res.* **2000**, *28*, 235–242.
[33] L. Bräuer, W. Brandt, L. A. Wessjohann, *J. Mol. Model.* **2004**, *10*, 317–327.
[34] M. N. Ashby, S. Y. Kutsunai, S. Ackerman, A. Tzagoloff, P. A. Edwards, *J. Biol. Chem.* **1992**, *267*, 4128–4136.
[35] M. Melzer, L. Heide, *Biochim. Biophys. Acta Lipids Lipid Metab.* **1994**, *1212*, 93–102.
[36] M. Takagi, M. Nishioka, H. Kakihara, M. Kitabayashi, H. Inoue, B. Kawakami, M. Oka, T. Imanaka, *Appl. Environ. Microbiol.* **1997**, *63*, 4504–4510.
[37] J. Cline, J. C. Braman, H. H. Hogrefe, *Nucleic Acids Res.* **1996**, *24*, 3546–3551.
[38] D. J. Sharkey, E. R. Scalice, K. G. Christy, S. M. Atwood, J. L. Daiss, *BioTechnology* **1994**, *12*, 506–509.
[39] K. Momose, H. Rudney, *J. Biol. Chem.* **1972**, *247*, 3930–3940.
[40] A. J. Chen, P. A. Kroon, C. D. Poulter, *Protein Sci.* **1994**, *3*, 600–607.
[41] A. Tachibana, Y. Yano, S. Otani, N. Nomura, Y. Sako, M. Taniguchi, *Eur. J. Biochem.* **2000**, *267*, 321–328.
[42] S. C. Trapp, R. B. Croteau, *Genetics* **2001**, *158*, 811–832.
[43] J. Pandit, D. E. Danley, G. K. Schulte, S. Mazzalupo, T. A. Pauly, C. M. Hayward, E. S. Hamanaka, J. F. Thompson, H. J. Harwood, *J. Biol. Chem.* **2000**, *275*, 30610–30617.
[44] C. A. Lesburg, G. Z. Zhai, D. E. Cane, D. W. Christianson, *Science* **1997**, *277*, 1820–1824.
[45] A. Andreeva, D. Howorth, S. E. Brenner, T. J. P. Hubbard, C. Chothia, A. G. Murzin, *Nucleic Acids Res.* **2004**, *32*, D226–D229.
[46] *Prime 1.2, Protein Structure Prediction Suite, 2005*, Schrödinger, LLC, New York, USA, **2005**.
[47] D. W. Christianson, *Chem. Rev.* **2006**, *106*, 3412–3442.
[48] P. H. Liang, T. P. Ko, A. H. J. Wang, *Eur. J. Biochem.* **2002**, *269*, 3339–3354.
[49] J. Cheng, A. Z. Randall, M. J. Sweredoski, P. Baldi, *Nucleic Acids Res.* **2005**, *33*, W72–W76.
[50] C. M. Starks, K. W. Back, J. Chappell, J. P. Noel, *Science* **1997**, *277*, 1815–1820.
[51] K. Bryson, L. J. McGuffin, R. L. Marsden, J. J. Ward, J. S. Sodhi, D. T. Jones, *Nucleic Acids Res.* **2005**, *33*, W36–W38.
[52] L. J. McGuffin, K. Bryson, D. T. Jones, *Bioinformatics* **2000**, *16*, 404–405.
[53] D. T. Jones, W. R. Taylor, J. M. Thornton, *FEBS Lett.* **1994**, *339*, 269–275.

[54] D. T. Jones, W. R. Taylor, J. M. Thorton, *Biochemistry* **1994**, *33*, 3038–3049.
[55] D. T. Jones, *FEBS Lett.* **1998**, *423*, 281–285.
[56] R. A. Laskowski, M. W. Macarthur, D. S. Moss, J. M. Thornton, *J. Appl. Crystallogr.* **1993**, *26*, 283–291.
[57] M. P. Jacobson, D. L. Pincus, C. S. Rapp, T. J. F. Day, B. Honig, D. E. Shaw, R. A. Friesner, *Proteins Struct. Funct. Bioinf.* **2004**, *55*, 351–367.
[58] A. D. MacKerell, D. Bashford, M. Bellott, R. L. Dunbrack, J. D. Evanseck, M. J. Field, S. Fischer, J. Gao, H. Guo, S. Ha, D. Joseph-McCarthy, L. Kuchnir, K. Kuczera, F. T. K. Lau, C. Mattos, S. Michnick, T. Ngo, D. T. Nguyen, B. Prodhom, W. E. Reiher, B. Roux, M. Schlenkrich, J. C. Smith, R. Stote, J. Straub, M. Watanabe, J. Wiorkiewicz-Kuczera, D. Yin, M. Karplus, *J. Phys. Chem. B* **1998**, *102*, 3586–3616.
[59] E. Pellegrini, M. J. Field, *J. Phys. Chem. A* **2002**, *106*, 1316–1326.
[60] *MOE (The Molecular Operating Environment) Version 2006.08*, Chemical Computing Group, Inc., Montréal, Canada, **2007**.
[61] M. J. Sippl, *J. Mol. Biol.* **1990**, *213*, 859–883.
[62] M. Fulhorst, L. Wessjohann, **2007**; unpublished results.
[63] S. Ghosh, S. J. Lee, K. Ito, K. Akiyoshi, J. Sunamoto, Y. Nakatani, G. Ourisson, *Chem. Commun.* **2000**, 267–268.
[64] G. Pozzi, V. Birault, B. Werner, O. Dannenmuller, Y. Nakatani, G. Ourisson, S. Terakawa, *Angew. Chem. Int. Ed. Engl.* **1996**, *35*, 177–180; *Angew. Chem.* **1996**, *108*, 190–192.
[65] S. Takajo, H. Nagano, O. Dannenmuller, S. Ghosh, A. M. Albrecht, Y. Nakatani, G. Ourisson, *New J. Chem.* **2001**, *25*, 917–929.
[66] J. A. Hamilton, G. B. Cox, *Biochem. J.* **1971**, *123*, 435–443.
[67] *Jaguar 6.0*, Schrödinger, LLC, New York, USA, **2007**.
[68] V. J. Davisson, A. B. Woodside, T. R. Neal, K. E. Stremler, M. Muehlbacher, C. D. Poulter, *J. Org. Chem.* **1986**, *51*, 4768–4779.
[69] J. Cline, J. C. Braman, H. H. Hogrefe, *Nucleic Acids Res.* **1996**, *24*, 3546–3551.
[70] M. Siebert, A. Bechthold, M. Melzer, U. May, U. Berger, G. Schroder, J. Schroder, K. Severin, L. Heide, *FEBS Lett.* **1992**, *307*, 347–350.
[71] G. Jones, P. Willett, R. C. Glen, *J. Comput.-Aided Mol. Des.* **1995**, *9*, 532–549.
[72] G. Jones, P. Willett, R. C. Glen, A. R. Leach, R. Taylor, *J. Mol. Biol.* **1997**, *267*, 727–748.
[73] J. W. M. Nissink, C. Murray, M. Hartshorn, M. L. Verdonk, J. C. Cole, R. Taylor, *Proteins Struct. Funct. Genet.* **2002**, *49*, 457–471.
[74] M. L. Verdonk, J. C. Cole, M. J. Hartshorn, C. W. Murray, R. D. Taylor, *Proteins Struct. Funct. Genet.* **2003**, *52* 609–623.
[75] *Pymol 2007*, DeLano Scientific, LLC, South San Francisco, USA, **2007**.
[76] *MOLCAD (MOLecular Computer Aided Design)*, J. Brickmann et al., TU Darmstadt; Germany.
[77] SYBYL 7.0. 2007. Tripos, Inc., 1699 South Hanley Rd., St. Louis, MO 63144-62917.

Received: September 28, 2007
Published online on March 13, 2008

